# MODELING THE TRANSVERSE THERMAL CONDUCTIVITY OF 2-D $SiC_f$/SiC COMPOSITES MADE WITH WOVEN FABRIC

GERALD E. YOUNGBLOOD,* DAVID J. SENOR, and RUSSELL H. JONES
*Pacific Northwest National Laboratory, P.O. Box 999, MSIN P8-15, Richland, Washington 99352*

Received October 1, 2003
Accepted for Publication January 24, 2004

*The hierarchical two-layer (H2L) model describes the effective transverse thermal conductivity ($k_{eff}$) of a two-dimensional (2-D) $SiC_f$/SiC composite plate made from stacked and infiltrated woven fabric layers in terms of constituent properties and microstructural and architectural variables. The H2L model includes the effects of fiber-matrix interfacial conductance, high-fiber packing fractions within individual tows, and the nonuniform nature of 2-D fabric/matrix layers that usually include a significant amount of interlayer porosity. Previously, H2L model $k_{eff}$ predictions were compared to measured values for two versions of 2-D Hi-Nicalon™/pyrocarbon (PyC)/isothermal chemical vapor infiltration (ICVI)-SiC composite, one with a "thin" (0.11-μm) and the other with a "thick" (1.04-μm) PyC fiber coating, and for a 2-D Tyranno™ SA/thin PyC/forced flow chemical vapor infiltration SiC composite. In this study, H2L model $k_{eff}$ predictions were compared to measured values for a 2-D $SiC_f$/SiC composite made using the ICVI process with Hi-Nicalon type S fabric and a thin PyC fiber coating. The values of $k_{eff}$ determined for the latter composite were significantly greater than the $k_{eff}$ values determined for the composites made with either the Hi-Nicalon or the Tyranno SA fabrics. Differences in $k_{eff}$ values were expected for the different fiber types, but major differences also were due to observed microstructural and architectural variations between the composite systems, and as predicted by the H2L model.*

**KEYWORDS:** *thermal conductivity, ceramic matrix composite, silicon carbide*

## I. INTRODUCTION

Recent fusion reactor design concepts utilizing continuous fiber-reinforced $SiC_f$/SiC composite as a structural material require a net through-thickness or "effective" thermal conductivity ($k_{eff}$) equal to 15 to 20 W/mK during operation in the temperature range 600 to 1000°C (Ref. 1). The thermal conductivity of monolithic SiC made by chemical vapor deposition (CVD) (CVD-SiC) was shown to decrease by ~90% or 70% of unirradiated values after neutron irradiation above saturation doses at 600 and 1000°C, respectively. For $SiC_f$/SiC made with Nicalon™ CG fabric and by the isothermal chemical vapor infiltration (ICVI) process the decrease was less, ~65% or 45%, respectively.[2] The degradation in $k_{eff}$ for $SiC_f$/SiC composites made by chemical vapor infiltration (CVI) and with advanced SiC fiber generally has been observed to fall between these boundary values.[3] Based on these observed degradation limits, to meet current fusion thermal conductivity goals, we estimate that candidate $SiC_f$/SiC composites should have unirradiated $k_{eff}$ values of 43 and 27 W/mK minimum at 600 and 1000°C, respectively. Current commercially available composites made by CVI processing with Hi-Nicalon SiC fabric exhibit $k_{eff}$ values at 600 and 1000°C of ~11 and 9 W/mK, respectively.[3] These values fall far short of fusion concept design goals. Introduction of advanced, near-stoichiometric crystalline SiC fibers with relatively high fiber thermal conductivity values (particularly, Hi-Nicalon type S from Nippon Carbon, Ltd., ≈20 W/mK, and Tyranno™ SA from Ube Industries, Ltd., 45 to 65 W/mK at ambient) compared to Hi-Nicalon (≈7 W/mK at ambient) promise some possibility of improving $k_{eff}$ values.[4] Processing strategies other than CVI [e.g., melt infiltration, hybrid PIP-CVR, reaction sintering, and LPS-NITE (Refs. 5 through 8, respectively)] also have indicated some promise. Recently, $SiC_f$/SiC made with a three-dimensional (3-D) architectural scheme and exhibiting a marked increase in $k_{eff}$ was reported.[9] Another 3-D scheme that introduces a particularly high *K*-value fiber (such as Amoco K1100™ graphite fiber with $K_f \approx$ 400 W/mK at 600°C) into the through-thickness direction also is being investigated.[10]

To better understand the overall degradation of $k_{eff}$ in irradiated $SiC_f$/SiC composites, the degradation in the thermal conductivity of the individual composite

*E-mail: ge.youngblood@pnl.gov

constituents (fiber, matrix, and fiber coating) must be evaluated. Because neither the fiber coating nor the matrix constituent thermal conductivity values can be separately measured in the composite, reliance on a realistic model must be used to infer their values. Degradation mechanisms of the individual composite constituents can then be analyzed from these inferred values. Unfortunately, recently developed models usually describe the thermal conductivity for simple structures (i.e., one-dimensional uniaxial), but not for two-dimensional (2-D) $SiC_f$/SiC structures with woven fabric architectures containing considerable porosity (e.g., 10 to 15% in CVI-processed composites). Furthermore, the shape and orientation as well as the amount of the porosity likely have a major influence on $k_{eff}$.

In previous work, the Hasselman-Johnson[11] (H-J) or the Markworth[12] models were used to predict $k_{eff}$ for a hypothetical composite made with initially high-conductivity fiber and matrix components before and after irradiation.[13] The H-J model included the effect of the fiber/matrix (f/m) interfacial conductance, which in a composite with numerous f/m interfaces can have a profound influence on $k_{eff}$. The Markworth model specifically included the effects of the fiber coating thickness and thermal conductivity. However, neither model explicitly contained the effects of porosity or the matrix and fabric layer distributions. In this work, a hierarchical two-layer (H2L) model is described that depends upon the fiber, fiber coating, and matrix "intrinsic" thermal conductivity values, as well as the effects of the fabric interlayer macroporosity, the fiber intrabundle microporosity, the actual fiber distribution within the fabric layers, and the overall matrix and fabric layer distributions.

Initially, the model that contained the effects of the f/m interfaces but not the effects of porosity and architectural factors was applied to measured values of $k_{eff}$ for two 2-D $SiC_f$/SiC systems made with Hi-Nicalon fabric layers and a CVI-SiC matrix.[14] Later, the H2L model was introduced and used to update the predictions for the same Hi-Nicalon composite systems.[15] An H2L-model analysis then was carried out and reported for measured values of $k_{eff}$ for a Tyranno SA composite system made by the forced flow CVI (FCVI) process.[16] In this paper, new data for a similar composite system, except made with Hi-Nicalon type S fabric, will be presented and analyzed using the H2L model. Then, the results will be compared for all three composite systems made with different fiber types and different architectures.

## II. H2L MODEL DESCRIPTION

In the H2L model, the composite architecture is represented by parallel fabric/CVI-SiC composite layers alternating in series with pure matrix CVI-SiC layers. The matrix CVI-SiC layers contain considerable amounts of laminar-shaped macroporosity, typically oriented with the laminar faces mostly parallel to the layers. The fabric/CVI-SiC composite layers contain needlelike, intrabundle porosity aligned parallel to the fibers. Either the H-J or the Markworth models are used to describe the f/m interfacial and/or the fiber coating effects within the fabric/CVI-SiC layers. A Maxwell-Eucken (ME) correction factor is used to describe the effects of porosity content, shape, and orientation within both the fabric/matrix and the fiber-free matrix layers.[17] A more detailed description of the H2L model is given in Ref. 15.

Briefly, the series model that describes the steady-state heat flow perpendicular to parallel alternating fabric and matrix layers is given by

$$1/k_{eff} = f_F/K_F + f_M/K_M \ , \tag{1}$$

where

$f_F, f_M$ = relative volumes of the fabric and matrix layers, respectively

$K_F, K_M$ = layer effective thermal conductivity values, respectively.

The ME correction factor (given in brackets) is used to obtain $K_M$ from $K_m$:

$$K_M = K_m\{(1-P)/(1+\beta P)\} \ , \tag{2}$$

where

$K_m$ = "intrinsic" matrix thermal conductivity without porosity

$P$ = macroporosity volume content of the fiber-free matrix layer

$\beta$ = macroporosity shape factor (e.g., when conduction within pores is temperature independent, $\beta \approx 1$ for needle-shaped pores aligned perpendicular to the heat flux, $\beta = \frac{1}{2}$ for isolated spherical pores, and $\beta > \frac{1}{2}$ for oblate ellipsoidal-shaped pores with their shorter axis aligned parallel to the heat flux).[17]

If the H-J model is used, $K_F$ is given by

$$K_F = K_m\{(1-P')/(1+\beta' P')\} \times [1-(B/A)f_p][1+(B/A)f_p]^{-1} \ , \tag{3}$$

where the term in brackets is the ME correction factor for the fabric layer that involves the fabric layer microporosity content and shape factors ($P'$ and $\beta'$, respectively). When the H-J model is used, the terms in braces are

$$A = 1 + K_f/ah + K_f/K_m$$

and

$$B = 1 + K_f/ah - K_f/K_m \ ,$$

where

$K_f$ = fiber thermal conductivity

$ah$ = product of the fiber radius $a$ and f/m interfacial conductance $h$

$f_p$ = average fiber packing fraction within the fabric layers.

If desired, the H-J terms in braces may be replaced by the Markworth model expressions, which are somewhat more complex.[15] The Markworth model better describes a composite when the fibers have a rather thick (>0.5 $\mu$m), thermally well-coupled fiber coating; the H-J model is better when the fiber coating is thin or the f/m interface exhibits debonding (thermal decoupling). For thin fiber coatings, the H-J and Markworth models give equivalent predictions if the substitution $h = K_c/t$ ($K_c$ and $t$ are the fiber coating thermal conductivity and thickness, respectively) is used.[16]

To determine the $P$ and $P'$ porosity factors in Eqs. (2) and (3), it is easiest to first calculate the average composite porosity $P_{avg}$ from the values of the measured composite bulk density $\rho_b$, the density of the matrix without macroporosity $\rho_m$, and the theoretical composite density $\rho_o$. Thus, where $f_f$ is the overall fiber volume fraction, $\rho_c$ is the fiber coating density, and $\rho_f$ and $D_f$ are fiber bulk density and average diameter, respectively; the average composite porosity is calculated as follows:

$$P_{avg} = (\rho_o - \rho_b)/\rho_m \ . \quad (4)$$

In Eq. (4), $\rho_o$ is estimated by

$$\rho_o \approx \rho_m - f_f[(\rho_m - \rho_f) + (4t/D_f)(\rho_m - \rho_c)] \ , \quad (5)$$

and $\rho_m$ is taken to be 3.20 g/cm$^3$ for dense SiC.

## III. EXPERIMENTAL

A composite plate (15 × 23 cm$^2$, 0-90 layup) was fabricated by GE Power Systems Composites[a] using six plies of five harness satin (5HS)–weave Hi-Nicalon type S fabric.[b] The properties for the type S fiber given by the manufacturer were as follows: density, 3.0 g/cm$^3$; tensile strength, 2.8 GPa; tensile modulus, 380 GPa; and oxygen content, 0.7 wt%. A pyrocarbon (PyC) fiber coating (nominally 150 nm thick) was applied by CVD to the fabric layup prior to SiC matrix infiltration by the isothermal CVI process. The nominal bulk density of the plate was 2.69 g/cm$^3$.

[a]GE Power Systems Composites was formerly DuPont Lanxide and then Honeywell Advanced Composites, Inc.

[b]The fabric was 18 epi, 500 filaments/yarn, lot number SCS0102, manufactured by Nippon Carbon Company in December 2001.

Eight thermal diffusivity disk samples (0.171 mm × 9.00-mm diameter with bulk density values ranging from 2.60 to 2.74 g/cm$^3$) were cored from the center portion of the plate. The samples were mounted four at a time in an Anter™ laser flash diffusivity system, and the thermal diffusivity $\alpha$ was measured for each sample in air from room temperature up to 400°C by procedures described previously.[18] Measurements were taken directly on the as-fabricated, somewhat rough surfaces of the disk samples. The standard method was used to calculate $k_{eff} = \alpha\rho_b C_p$. In this expression, $\alpha$ was estimated as a function of temperature up to 1000°C from the linear fit of the reciprocal thermal diffusivity versus room temperature to 400°C temperature data. Likewise, $\rho_b$ for each disk was determined up to 1000°C by weighing and dimensioning at room temperature and correcting for thermal expansion. The heat capacity $C_p$ as a function of temperature was determined by using a rule of mixtures. The thermal conductivity of the fiber $K_f(T)$ was separately measured using the same equipment by a related thermal diffusivity method.[4] Several pieces adjoining the thermal diffusivity disks were ground flat perpendicular to the composite layers and polished for microstructural examination. The fractions of fabric and matrix layer material; the fiber packing fraction; and the porosity content, orientation, and shape factors for the layers were estimated from a number of scanning electron microscopy (SEM) micrographs of the polished surfaces using the backscatter electron mode to enhance atomic number contrast between fiber, fiber coating, and matrix constituents.

## IV. RESULTS

In Fig. 1a, the measured thermal diffusivity data for each disk sample of the Hi-Nicalon type S composite from room temperature up to 400°C are given. The data points represent average values for five different laser shots at each temperature. The sample-to-sample scatter (within about a ±10% band) did not correlate with bulk density for the different samples. Rather, this scatter most likely was due to differences in the microstructural variables between individual samples. In Fig. 1b, the calculated average $k_{eff}$ values as a function of temperature for the Hi-Nicalon type S composite are compared to $k_{eff}$ values determined previously for similarly processed composites except made with Hi-Nicalon and Tyranno SA fabrics.[15,16] For the type S composite, the $k_{eff}$ values varied from a maximum value of ≈28 W/mK at 100°C down to a value of ≈14 W/mK at 1000°C and were significantly greater than similarly determined values for either the Tyranno SA or the Hi-Nicalon composites.

## V. ANALYSIS

In Figs. 2a and 2b, typical microstructures as viewed by SEM are given for the Hi-Nicalon type S composite

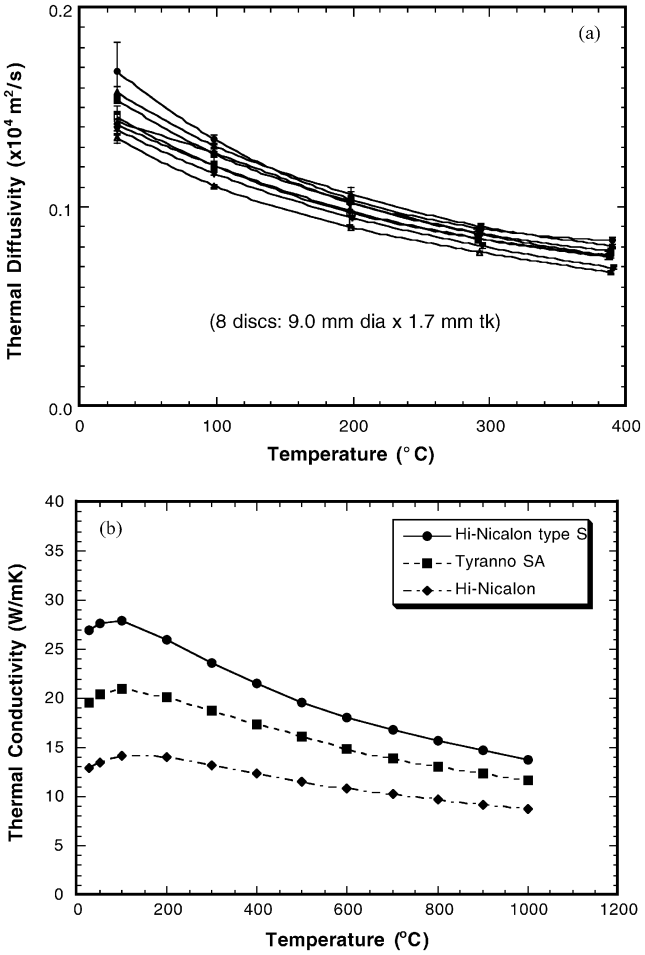


Fig. 1. (a) Measured thermal diffusivity values for eight disk samples cut from a 2-D $SiC_f$/SiC plate made from Hi-Nicalon type S fabric with a thin PyC fiber coating and ICVI-SiC matrix and (b) the average $k_{eff}$ calculated from the thermal diffusivity data shown in (a). For comparison, the $k_{eff}$ values determined for similarly fabricated 2-D $SiC_f$/SiC composites except made with either Hi-Nicalon or Tyranno SA fabric replacing the Hi-Nicalon type S fabric[15,16] also are shown.

and the Tyranno SA composite, respectively. Similar views of the microstructures for the two Hi-Nicalon systems are given in Ref. 15. Unfortunately, the contrast between the fiber and matrix components is poor for the Tyranno SA and Hi-Nicalon type S composites even when using the backscatter electron SEM mode because both components are essentially pure SiC. In contrast, for the Hi-Nicalon composite, the fiber and matrix components were easily separated because there was sufficient atomic number contrast. However, for all four composite systems at higher magnifications, the PyC fiber coating was very discernible, and its thickness was easily measured when using the backscatter electron SEM mode. The most striking observation is that in comparison to the Tyranno SA system with a 2-D plain-woven (PW), 0-30-60 fabric layup architecture, the macroporosity in the Hi-Nicalon type S composite with a 5HS-woven, 0-90 fabric layup architecture appears to be less lamellar in shape.

In Table I, measured structural and microstructural data for the 2-D $SiC_f$/SiC composites made with the three different woven fabrics (Hi-Nicalon, Tyranno SA, and Hi-Nicalon type S) are given. The fiber diameter and density ($D_f$ and $\rho_f$, respectively) are nominal values for each fiber type. The composite bulk density is an average value determined from measured density values for the thermal diffusivity samples in each system. The quantities $t$, $f_M$, and $f_p$ are average values for each system determined directly from a number of representative SEM micrographs similar to Figs. 2a and 2b. The porosity ellipticity factor $\varepsilon$ is calculated from $\varepsilon = c/a$, where $c$ and $a$ are macropore heights and extents, respectively. Representative $c$ and $a$ values were determined for each system by making direct measurements on 25 or more macropore footprints, again as exhibited in several SEM cross-sectional views similar to Figs. 2a and 2b taken at different locations. The quantity $P_M$ is the overall interlayer macroporosity volume fraction within the fiber-free matrix layers. An average value of $P_M$ was determined by measuring the macroporosity silhouette areas from several SEM micrographs. The ranges of values estimated

TABLE I

Structural, Microstructural, and Architectural Data for the 2-D $SiC_f$/SiC Composite Systems Made by the CVI Process with Hi-Nicalon, Tyranno SA, and Hi-Nicalon Type S Woven Fabrics

| System | $D_f$ ($\mu$m) | $\rho_f$ (g/cm$^3$) | $t$ ($\mu$m) | $\rho_b$ (g/cm$^3$) | $f_M$ (SEM) | $f_p$ (SEM) | $\varepsilon$ (SEM) | $P_M$ (SEM) | Weave |
|---|---|---|---|---|---|---|---|---|---|
| Hi-Nicalon-1 | 13.8 | 2.74 | 0.110 | 2.597 | 0.294 | 0.650 | 0.17 | 0.107 | PW |
| Hi-Nicalon-2 | 13.8 | 2.74 | 1.044 | 2.627 | 0.314 | 0.670 | 0.17 | 0.062 | PW |
| Tyranno SA | 10.0 | 3.02 | 0.190 | 2.667 | 0.262 | 0.577 | 0.12 | 0.105 | PW |
| Hi-Nicalon S | 12.0 | 3.00 | 0.188 | 2.710 | 0.173 | 0.502 | 0.17 | 0.065 | 5HS |
| Range | ±1.8 | ±0.02 | ±0.04 | ±0.02 | ±0.07 | ±0.06 | ±0.05 | ±0.007 | |

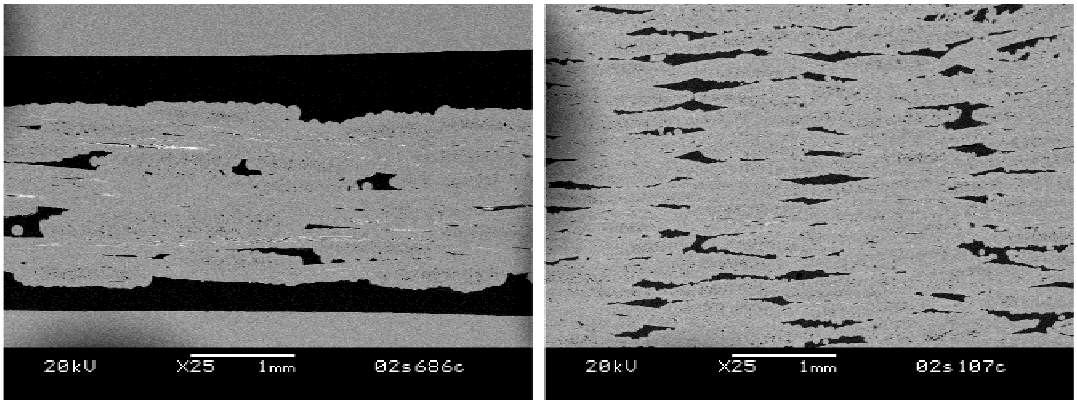


Fig. 2. SEM micrographs (backscatter electron mode) of polished cross sections comparing typical macroporosity content, orientation, and shape for (a) 2-D 5HS-woven, 0-90 fabric layup Hi-Nicalon type S and (b) 2-D PW, 0-30-60 fabric layup Tyranno SA $SiC_f$/SiC.

for the different parameters were determined from several independent measurements of each quantity.

In Table II, the calculated structural and microstructural factors used to calculate $k_{eff}$ [Eqs. (1) through (5)] are presented along with representative ranges of values. The quantity $\rho_o$ was calculated for each system by using Eq. (5) with the matrix density $\rho_m = 3.20$ g/cm$^3$ for $\beta$-SiC and the fiber coating density $\rho_c = 1.9$ g/cm$^3$ for CVD-applied PyC. In this calculation, the nominal fiber volume fraction $f_f$ was assumed to be 0.4 for each system except for the Tyranno SA system where $f_f = 0.37$ (Ref. 19). Then, the quantity $P_{avg}$ was calculated using Eq. (4) with $\rho_b$ given in Table I. The fractional fabric content $f_F$ was calculated as the difference $1 - f_M$ ($f_M$ given in Table I). The porosity content $P$ used in the ME correction factor for the matrix layers in Eq. (2) was estimated by $P = P_M/f_M$ ($P_M$ and $f_M$ given in Table I). Because the interlayer macroscopic porosity content was assigned to the matrix layers, the value determined from SEM micrographs $P_M$ was adjusted by dividing by $f_M$. Similarly, the fabric layer porosity content $P'$ used in the ME correction in Eq. (3) was estimated by $P' = (P_{avg} - P_M)/f_F$. Finally, the porosity shape and orientation factor $\beta$ used in the ME correction to obtain $K_M$ in Eq. (2) was estimated for each system by Marino's method[17] from the representative macroporosity ellipticity factor $\varepsilon$ given in Table I. In Marino's method, the macroporosity is assumed to have an oblate ellipsoidal shape. However, for the $K_F$ calculation, $\beta' \approx 1$ in the ME correction because the fabric micropores were needlelike with their lengths perpendicular to the heat-flow direction.

Although the uncertainty range estimates are rather large for the structural and microstructural factors listed in Tables I and II, the following trends are revealed. First, the Hi-Nicalon type S composite had the highest bulk density and lowest intrabundle packing fraction of the four systems. Likewise, the type S composite had the highest fabric layer fraction. Finally, the Hi-Nicalon type S system with 2-D 5HS fabric layers in a 0-90 layup pattern had macroporosity with relatively high ellipticity (low $\beta$ values) compared to the Tyranno SA system with 2-D PW fabric layers in a 0-30-60 layup pattern.

TABLE II

Calculated Structural and Microstructural Factors for Composite Systems Listed in Table I

| System | $\rho_o$ (g/cm$^3$) Eq. (5) | $P_{avg}$ Eq. (4) | $f_F$ Eq. (1) | $P$ Eq. (2) | $P'$ Eq. (3) | $\beta$ Eq. (2) | $\beta'$ Eq. (3) |
|---|---|---|---|---|---|---|---|
| Hi-Nicalon-1 | 2.999 | 0.126 | 0.706 | 0.36 | 0.027 | 1.3 | 1 |
| Hi-Nicalon-2 | 2.859 | 0.073 | 0.686 | 0.20 | 0.015 | 1.3 | 1 |
| Tyranno SA | 3.097 | 0.134 | 0.738 | 0.40 | 0.039 | 1.6 | 1 |
| Hi-Nicalon S | 3.087 | 0.118 | 0.827 | 0.38 | 0.031 | 1.3 | 1 |
| Range | ±0.02 | ±0.01 | ±0.07 | ±0.08 | ±0.005 | ±0.4 | ±0.1 |

In Figs. 3a through 3d, the predicted values of $K_c$, $K_m$, $K_M$, and $K_F$ are shown as a function of temperature when using the H2L model based on the structural and microstructural factors listed in Tables I and II and the measured values of $K_f$ and $k_{eff}$. The $K_f(T)$ values were reported earlier in Ref. 4. By requiring that both Hi-Nicalon systems with similarly fabricated ICVI-SiC matrix have the same values of $K_m$, a fairly reliable estimate of $K_c$ was extracted by an iteration method. This was done by varying $K_c$ for the Hi-Nicalon-2 ("thick" PyC) system until the $k_{eff}$ values predicted by the H2L model matched measured values of $k_{eff}$. For this case (Fig. 3b), the Markworth model, which explicitly depends on the fiber coating $K_c$ and $t$ values, was used. The derived $K_c$ values were then assigned to the other three systems with "thin" interfaces and "good" f/m thermal coupling (Figs. 3a, 3c, and 3d).

The H-J model is not that sensitive to having the exact values of $K_c$ for composites with thin interfaces, so using approximate values was acceptable for curve-fitting purposes. Then, the H-J model was used to calculate $K_F$ by Eq. (3) for these systems. Finally, $K_m$ values were varied for the Tyranno SA and Hi-Nicalon type S systems until the $k_{eff}$ values predicted by the H2L model matched experimentally measured values of $k_{eff}$. The derived values of $K_m$ were then used to calculate $K_M$ by Eq. (2).

As shown in Figs. 3a through 3d, $K_c$ ranged from ≈28 W/mK at room temperature, increased to a maximum 34 W/mK at about 300°C, and then decreased slightly to ≈28 W/mK at 1000°C. Meanwhile, "intrinsic" $K_m$ values derived for both Hi-Nicalon systems and the Hi-Nicalon type S system were approximately the same, with a maximum value of ≈40 W/mK at room temperature and decreasing continuously to 18 to 20 W/mK at 1000°C. These values were expected to be similar because the matrix for these three systems was fabricated by the same ICVI process. In contrast, the derived $K_m$

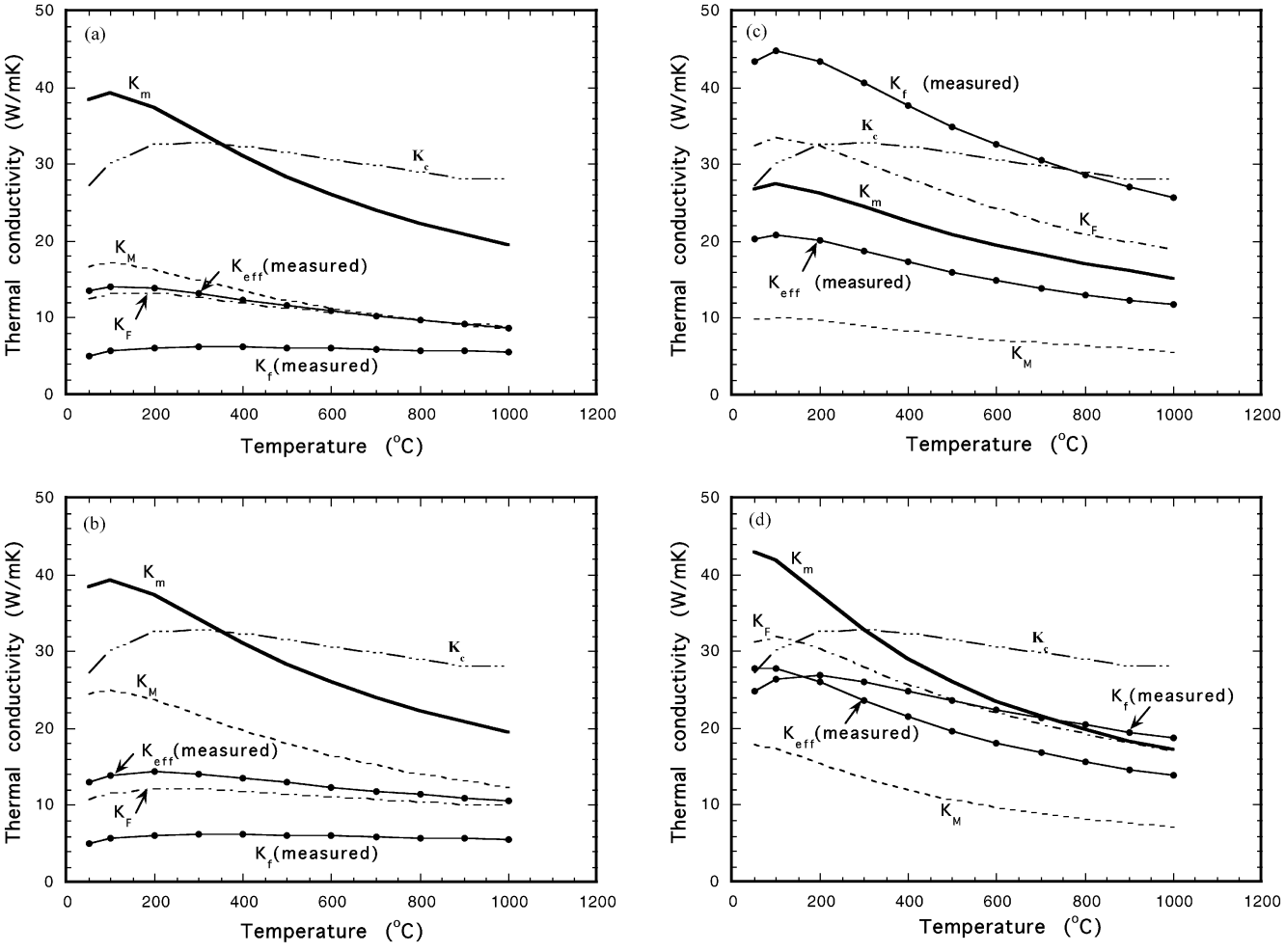


Fig. 3. H2L model predictions for $K_c$, $K_m$, $K_M$, and $K_F$ based on measured values of $K_f$ and $k_{eff}$ for four systems: (a) Hi-Nicalon/thin PyC/ICVI-SiC, (b) Hi-Nicalon/thick PyC/ICVI-SiC, (c) Tyranno SA/thin PyC/FCVI-SiC, and (d) Hi-Nicalon type S/thin PyC/ICVI-SiC. Note that $K_c(T)$ was assumed to be the same for all four composite systems.

values for the Tyranno SA system appeared to be somewhat lower, with a maximum value of ≈28 W/mK at room temperature and decreasing continuously to ≈15 W/mK at 1000°C. Apparently, the "intrinsic" $\beta$-SiC matrix formed by the FCVI process had a lower thermal conductivity than that formed by the ICVI process. This could be due to detailed microstructural differences caused by the differences in the rate of SiC deposition or in the deposition temperature for the two processes. The ICVI matrix was formed over a period of ~1 month, while the FCVI matrix was formed in a few days. For the particular Tyranno SA composite examined, the low values of $K_M$ reflect both the relatively low values of $K_m$ and the higher macropore shape factor $\beta$.

In Table III, according to the H2L model, the relative change in $k_{eff}$ for a 10% change for each parameter that increases $k_{eff}$ is listed. These changes were based on the data for the Hi-Nicalon-1 system where the changes in $k_{eff}$ were the largest of the four systems, and therefore the most sensitive.

According to Table III, increasing the matrix or fiber thermal conductivity values or decreasing the matrix macroporosity content are the most important for affecting an increase in $k_{eff}$. If $K_f < K_m$, obviously decreasing the fiber content also is important, more so the larger the difference in $K$ values. The reverse situation occurs if $K_f > K_m$, in which case the fiber content must be increased to increase $k_{eff}$. Interestingly, increasing $K_c$ or decreasing $t$ appears to have little effect on $k_{eff}$. Part of the reason for this is that for the examined systems the f/m interfaces were well bonded; thus, the interface thermal conductance already was optimized. For example, for the Hi-Nicalon-1 system, $h \approx K_c/t \approx 3 \times 10^4$ W/cm$^2$ K, which is a value sufficiently high so that a further increase in $h$ would have little effect on $k_{eff}$ (Ref. 13). However, a decrease in $h$ by orders of magnitude can occur because of debonding (perhaps caused by mechanical stress, fatigue, or differential matrix swelling/fiber shrinkage during irradiation), in which case a relatively large effect (decrease) on $k_{eff}$ would be expected. If all the listed parameters together changed by 10% in a manner to increase $k_{eff}$, the net increase for the Hi-Nicalon composite system would be ~21% or 20% at 600 and 1000°C, respectively. The net increase for the Nicalon type S system would be less because $K_f \approx K_m$, and the net increases for the Tyranno SA and Hi-Nicalon systems would be similar because $K_f/K_m \approx K_m/K_f$ for these two systems, respectively.

TABLE III

Relative Change in $k_{eff}$ at 600 and 1000°C for 10% Change in Listed Parameter Values*

| Parameter | Value at 600°C | Percent Effect | Value at 1000°C | Percent Effect |
|---|---|---|---|---|
| $K_f$ (W/mK) | 6.04 | 3.4 | 5.57 | 3.5 |
| $K_m$ (W/mK) | 26.0 | 6.6 | 19.5 | 6.4 |
| $K_c$ (W/mK) | 30.6 | <0.1 | 28.6 | <0.1 |
| $t$ ($\mu$m) | 0.110 | <0.1 | 0.110 | <0.1 |
| $a$ ($\mu$m) | 7.0 | <0.1 | 7.0 | <0.1 |
| $P$ | 0.36 | 2.4 | 0.36 | 2.6 |
| $P'$ | 0.027 | 0.2 | 0.027 | 0.2 |
| $f_p$ | 0.65 | 7.0 | 0.65 | 5.8 |
| $\beta$ | 1.3 | 1.0 | 1.3 | 1.0 |
| Total | | 20.9 | | 19.8 |

*Based on the data for the Hi-Nicalon-1 (thin PyC interface) system.

As mentioned, for the composite systems considered, the Tyranno SA system was expected to have the highest $k_{eff}$ values because of the high values of $K_f$ for this system. However, the Hi-Nicalon type S system was observed to have $k_{eff}$ values ~25% higher than the values for the SA system even though $K_f$ values for type S fiber, depending on temperature, range from 40 to 60% lower than for the SA fiber. According to the H2L model, the lower $K_m$ values and the relatively high macroporosity shape factor for the SA system more than offset gains in $k_{eff}$ expected from using the SA fiber.

The Tyranno SA composite examined in this work was from a first-generation fabrication setup, which likely was responsible for its somewhat substandard macroporosity factors. By exchanging the SA $K_f$ values for the type S $K_f$ values in the H2L model for the type S composite, predictions for a "hypothetical" Tyranno SA composite with improved $K_m$ values and porosity factors and therefore improved $k_{eff}$ values can be simulated. That is, a high-conductivity fabric layer is then combined with a high-conductivity matrix layer with a reduced porosity influence to produce a composite system with optimized $k_{eff}$. The H2L model predictions of $k_{eff}$ for such a hypothetical composite are presented in Fig. 4 along with measured $k_{eff}$ values for the type S and SA systems.

According to the H2L model, by changing each controllable parameter (parameters listed in Tables I and II) by 10% in such a manner as to increase $k_{eff}$, the $k_{eff}$ values for the 10% optimized Tyranno SA system were only ~12 and 8% higher than corresponding $k_{eff}$ values for the hypothetical Tyranno SA system at 600 and 1000°C, respectively. Furthermore, the 10% optimized $k_{eff}$ values were significantly less (52 and 62%, respectively) than our projected current minimum fusion $k_{eff}$ goals for $SiC_f$/SiC at these temperatures.

For the following reasons, it does not appear likely that the current minimum fusion $k_{eff}$ goals can be attained for even an optimized 2-D $SiC_f$/SiC composite system made with woven fabrics with a CVI-SiC fabricated matrix. The Tyranno SA fiber is a relatively high purity, crystalline SiC fiber with about as high a value of $K_f$ achievable for a SiC-type fiber. The ICVI-SiC matrix is high-purity crystalline SiC with a minimum amount of

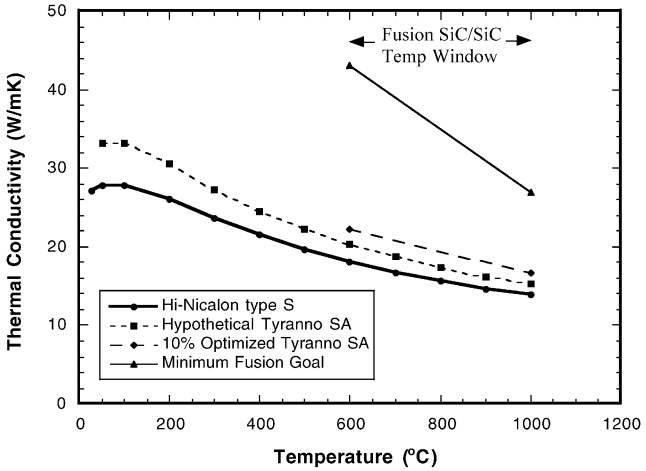


Fig. 4. H2L model predictions of $k_{eff}$ for a hypothetical Tyranno SA composite system and a 10% optimized Tyranno SA system compared to measured $k_{eff}$ values for the Hi-Nicalon type S and our projected minimum $k_{eff}$ fusion goals for unirradiated $SiC_f$/SiC, 43 and 27 W/mK at 600 and 1000°C, respectively.

internal microporosity and a favorable grain microstructure for producing relatively high $K_m$ values. A certain amount of macroporosity, both within the fiber bundles and between the fabric layers, is necessary for gas exchange as part of the CVI process and likely cannot be reduced beyond that obtained using the isothermal process. Using satin weave fabric with a 0-90 layup likely results in the most favorable macroporosity shape factor (low $\beta$ values) for a 2-D alternating fabric-matrix layer architecture. The f/m interfaces for these systems were all well bonded, so the interfacial conductance was already high enough to not have a degrading effect on $k_{eff}$. Overall, it appears that the margin of improvement in $k_{eff}$ required to meet the minimum fusion $k_{eff}$ goals is just too large (on the order of doubling even the optimized $k_{eff}$ values) to be met by any minor improvements potentially possible through CVI fabrication, structural, or architectural methods. Unless design considerations allow adjustment of the minimum fusion $k_{eff}$ goals downward, it appears prudent for the fusion community to emphasize the other methods listed in Sec. I for continued efforts to develop a $SiC_f$/SiC composite suitable to meet the fusion thermal conductivity goals for $SiC_f$/SiC.

## VI. SUMMARY AND CONCLUSIONS

Measured values of $k_{eff}$ as a function of temperature for three $SiC_f$/SiC composite systems made by similar CVI processing but with three different fiber types were analyzed using the H2L model. These systems were a Hi-Nicalon/thin PyC/ICVI-SiC composite and a Hi-Nicalon/thick PyC/ICVI-SiC composite with 0.110-$\mu$m and 1.044-$\mu$m PyC fiber coatings, respectively; a Tyranno SA/thin PyC/FCVI-SiC composite; and a Hi-Nicalon type S/thin PyC/ICVI-SiC composite. Because of the CVI processing, each system appeared to have good f/m thermal coupling. From the results of this analysis, we conclude the following:

1. The H2L model realistically describes how $k_{eff}$ for a 2-D composite made with stacked and infiltrated fabric layers depends upon structural, microstructural, and architectural variables as well as constituent fiber, matrix, and f/m interface properties.

2. The fiber PyC coating $K_c$ values predicted by the H2L model ranged from ≈28 W/mK at room temperature, increased to a maximum 34 W/mK at ~300°C, then continuously decreased to ≈28 W/mK at 1000°C. However, the $k_{eff}$ values predicted by the H2L model are relatively insensitive to the actual $K_c(T)$ values when the composite exhibits good f/m thermal coupling.

3. Likewise, the intrinsic $K_m$ values of an ICVI-SiC matrix predicted by the H2L model ranged from ≈40 W/mK at room temperature and decreased continuously to 18 to 20 W/mK at 1000°C. The corresponding $K_m$ values for the FCVI-SiC matrix were ≈28 W/mK at room temperature decreasing to ≈15 W/mK at 1000°C.

4. Measured $k_{eff}$ values for the composite system made with 5HS Hi-Nicalon type S fabric were higher than those for the system with PW Tyranno SA fabric even though $K_f$ for type S is less than $K_f$ for SA fiber. According to the H2L model, these differences can be attributed to the optimized macroporosity shape factor (low $\beta$ values) obtained by using the satin weave fabric with a 0-90 fabric layup architecture and to the favorable crystalline matrix microstructure obtained by using the ICVI rather than the FCVI process.

5. Nevertheless, the relatively high $k_{eff}$ values observed for the CVI-processed Hi-Nicalon type S system or even predicted for a hypothetical optimized 2-D Tyranno SA system fall far short of current fusion $k_{eff}$ goals for $SiC_f$/SiC (projected by this study to be 43 and 27 W/mK at 600 and 1000°C, respectively). Other strategies to attain the fusion $k_{eff}$ goals for $SiC_f$/SiC should be pursued.

## ACKNOWLEDGMENTS

The U.S. Department of Energy (DOE) Nuclear Energy Research Initiative funded the model development work, and US DOE Fusion Energy Materials funded the experimental work. Pacific Northwest National Laboratory is operated by Battelle for DOE under contract DE-AC06-76RLO1830.

## REFERENCES


1. A. R. RAFFRAY et al., "Design and Material Issues for High Performance $SiC_f$/SiC-Based Fusion Power Cores," *Fusion Eng. Des.*, **55**, 55 (2001).

2. D. J. SENOR, G. E. YOUNGBLOOD, C. E. MOORE, D. J. TRIMBLE, G. A. NEWSOME, and J. J. WOODS, "Effects of Neutron Irradiation on Thermal Conductivity of SiC-Based Composites and Monolithic Ceramics," *Fusion Technol.*, **30**, 943 (1996).

3. G. E. YOUNGBLOOD, D. J. SENOR, and R. H. JONES, "Thermal Diffusivity/Conductivity of Irradiated Hi-Nicalon™ 2D-$SiC_f$/SiC Composite," "Fusion Materials Semiannual Progress Report (FMSPR)," DOE/ER-0313/30, p. 41, U.S. Department of Energy (June 30, 2003).

4. G. E. YOUNGBLOOD and R. H. JONES, "An Update on the 'KFIB' Experiment," "Fusion Materials Semiannual Progress Report (FMSPR)," DOE/ER-0313/30, p. 64, U.S. Department of Energy (June 30, 2003).

5. R. T. BHATT, J. Z. GYEKENYESI, and J. B. HURST, "Silicon Effects on Properties of Melt-Infiltrated SiC/SiC Composites," *Ceram. Eng. Sci. Proc.*, **21**, *3*, 331 (2000).

6. W. KOWBEL, C. A. BRUCE, K. L. TSOU, K. PATEL, J. C. WITHERS, and G. E. YOUNGBLOOD, "High Thermal Conductivity SiC/SiC Composites for Fusion Applications," *J. Nucl. Mater.*, **283–287**, 570 (2000).

7. S. P. LEE, J. S. PARK, Y. KATOH, A. KOHYAMA, D. H. KIM, J. K. LEE, and H. K. YOON, "Process, Microstructure and Flexural Properties of Reaction Sintered Tyranno™ SA/SiC Composites," *J. Nucl. Mater.*, **307–311**, 1191 (2002).

8. Y. KATOH, S. DONG, and A. KOHYAMA, "A Novel Processing Technique of Silicon Carbide-Based Ceramic Composites for High Temperature Applications," *Ceram. Trans.*, **144**, 1191 (2002).

9. R. YAMADA, N. IGAWA, T. TAGUCHI, and S. JITSUKAWA, "Highly Thermal Conductive, Sintered SiC Fiber-Reinforced 3D-SiC/SiC Composites," *J. Nucl. Mater.*, **307–311**, 1215 (2002).

10. W. KOWBEL, A. TSOU, C. A. BRUCE, J. C. WITHERS, and G. E. YOUNGBLOOD, "High Thermal Conductivity SiC/SiC and Hybrid C/SiC-SiC Composites," *Proc. 5th IEA Workshop SiC/SiC Composites for Fusion Energy Applications*, San Diego, California, April 12–13, 2002, International Energy Agency.

11. D. P. H. HASSELMAN and L. F. JOHNSON, "Effective Thermal Conductivity of Composites with Interfacial Thermal Barrier Resistance," *J. Comp. Mater.*, **21**, 508 (1987).

12. A. J. MARKWORTH, "The Effective Thermal Conductivity of a Unidirectional Fibre Composite with Fiber-Matrix Debonding: A Calculation Based on Effective-Medium Theory," *J. Mater. Sci. Lett.*, **12**, 1487 (1993).

13. G. E. YOUNGBLOOD, D. J. SENOR, R. H. JONES, and S. GRAHAM, "The Transverse Thermal Conductivity of 2D-$SiC_f$/SiC Composites," *Comput. Sci. Technol.*, **62**, 1127 (2002).

14. G. E. YOUNGBLOOD, D. J. SENOR, R. H. JONES, and W. KOWBEL, "Optimizing the Transverse Thermal Conductivity of 2D-$SiC_f$/SiC Composites, II. Experimental," *J. Nucl. Mater.*, **307–311**, 1120 (2002).

15. G. E. YOUNGBLOOD, D. J. SENOR, and R. H. JONES, "Modeling the Transverse Thermal Conductivity of 2D-SiC/SiC Composites," "Fusion Materials Semiannual Progress Report (FMSPR)," DOE/ER-0313/31, p. 5 (Dec. 31, 2001).

16. G. E. YOUNGBLOOD, D. J. SENOR, and R. H. JONES, "Modeling the Transverse Thermal Conductivity of 2D-$SiC_f$/SiC Composites with Woven Architectures," *Proc. 5th IEA Workshop SiC/SiC Composites for Fusion Energy Applications*, San Diego, California, April 12–13, 2002, p. 36, International Energy Agency.

17. G. P. MARINO, "The Porosity Correction Factor for the Thermal Conductivity of Ceramic Fuels," *J. Nucl. Mater.*, **38**, 178 (1971).

18. D. J. SENOR, G. E. YOUNGBLOOD, D. V. ARCHER, C. E. MOORE, and C. E. CHAMBERLIN, "Recent Progress in Thermal Conductivity Testing of SiC-Based Materials for Fusion Reactor Applications," *Proc. 3rd IEA Workshop SiC/SiC Ceramic Composites for Fusion Structural Applications*, Cocoa Beach, Florida, January 29–30, 1999, International Energy Agency.

19. Y. KATOH, Private Communication.


---


**Gerald E. Youngblood** (BA, physics, University of California at Davis, 1962; PhD, physics, University of Utah, Salt Lake City, 1973) is senior research scientist at Pacific Northwest National Laboratory (PNNL). His current interests are fusion and nuclear reactor materials research.

**David J. Senor** (BS, 1988, and PhD, 1992, nuclear engineering, Texas A&M University) is staff engineer at PNNL. His current interests are fusion and fission reactor materials, nuclear fuels, refractory coatings, and ceramic joining.

**Russell H. Jones** (BS, metallurgy, California State Polytechnic College, 1967; PhD, materials science and engineering, University of California, Berkeley, 1971) is laboratory fellow at PNNL. His current interests are environmental effects on materials, stress corrosion, high-temperature composites, fracture, fusion materials, intermetallics, and lightweight automotive materials.